J Mater Sci (2008) 43:6999–7012
DOI 10.1007/s10853-008-3005-3

REVIEW

Review: degradation-induced embrittlement in semi-crystalline polymers having their amorphous phase in rubbery state

Bruno Fayolle · Emmanuel Richaud · Xavier Colin · Jacques Verdu

Received: 8 April 2008 / Accepted: 16 September 2008 / Published online: 18 October 2008

Abstract The literature dealing with degradation-induced embrittlement mechanisms in semi-crystalline polymers having their amorphous phase in rubbery state is reviewed. It is first demonstrated that the decrease of molar mass resulting from a quasi-homogeneous chain scission process is responsible for embrittlement. The main specificity of the polymer family under study is that embrittlement occurs at a very low conversion of the degradation process, while the entanglement network in the amorphous phase is slightly damaged. In these polymers, chain scission induces chemicrystallization. The analyses of available data on this process show that it is characterized by a relatively high yield: about one half entanglement strands integrate the crystalline phase after one chain scission. A simple relationship expressing the chemicrystallization yield for a given polymer structure is proposed. Chain scission and chemicrystallization can lead to embrittlement through two possible causal chains: (1) chain scission → molar mass decrease → chemicrystallization → decrease of the interlamellar spacing → embrittlement. (2) Chain scission → molar mass decrease → chemicrystallization → decrease of the tie-macromolecule concentration → embrittlement. At this state of our knowledge, both causal chains are almost undistinguishable.

B. Fayolle (✉) · E. Richaud · X. Colin · J. Verdu
LIM (UMR 8006), Arts et Métiers ParisTech., 151 boulevard de l'Hôpital, 75013 Paris, France
e-mail: bruno.fayolle@paris.ensam.fr

Introduction

In a wide variety of chemical aging causes, for instance photo-oxidation, thermo-oxidation, and hydrolysis, linear polymers undergo random chain scission which induces embrittlement. The latter can be described as a transition from a ductile to a brittle behavior, which displays the following characteristics:

1. It occurs suddenly and abruptly. This abrupt character is especially marked when the mechanical behavior is characterized by a tensile test [1], but no doubt, embrittlement corresponds to a critical structural state.
2. It occurs at low conversion of the degradation process, generally when less than 1% of the monomer units have undergone a chain scission. These conversions are generally out of reach of common spectrochemical methods (IR, NMR, etc.). This fact explains, at least partially, why embrittlement mechanisms remained an opened question for a long time and why interest of research workers had been mostly focused on chemical aspects of aging at high conversions. It is noteworthy that a ductile–brittle transition can also occur without chemical degradation in polymers submitted to mechanical loads during aging, for instance in the case of polyethylene (PE) pipes under pressure [2]. This important case will not be considered here, our investigation being focused only on chemical degradation effect.

As far as embrittlement mechanisms are concerned, semi-crystalline polymers having their amorphous phase in rubbery state such as PE, polypropylene (PP), polyoxymethylene (POM), etc., constitute a specific family because their embrittlement occurs at especially low conversions of the chain scission process. One can suspect that the chain

scission process induces morphological changes and that these latter play an important role as it will be seen next.

It is not uncommon to see articles reporting mechanical properties of aged polymers in the scientific and technical literature, but articles giving at the same time mechanical properties and pertinent analytical data needed for the understanding of embrittlement processes are very scarce. On the other hand, relatively little was known, until the end of the last century, on structure–fracture behavior relationships applied to aging cases. These factors can explain the relative under-development of the knowledge of embrittlement processes. The situation is now changing because there were decisive advances in the domain of polymer fracture properties in the last 15 years [3, 4]. It seemed to us interesting to use these advances to investigate on the links between the concerned domains, i.e. degradation-induced molar mass changes, morphological changes and consequences of these structural changes on the fracture behavior. Here, "degradation" is taken as synonym of "random chain scission".

This article has been written having in mind a more or less remote objective: the elaboration of a non-empirical kinetic model leading to lifetime prediction, using the ductile–brittle transition as an endlife criterion. The point of departure of this approach would be a model based on chemical kinetics principles and able to predict the number s of chain scissions. Examples of such models with relatively strong predictive power have been recently published in the case of unstabilized polymers [5, 6]. Their extension to the case of stabilized polymers is now under study in our laboratory [7]. It will be supposed here that the step of kinetic modeling of chemical degradation is solved and that the remaining issue can be summed up in the following question: Is it possible to imagine a causal chain starting from chain scission and leading to embrittlement, in which the elementary links would have a mathematical expression?

It seemed to us interesting to formulate the main problem relative to each link as a question and to dedicate one section to each question, in the order corresponding to the presumed causal chain: chain scission → decrease of molar mass → chemicrystallization → decrease of the interlamellar spacing → change of key morphology parameters → embrittlement.

Is molar mass a pertinent variable?

According to Griffith [8], the critical conditions for crack propagation in a solid would be given by:

$$\frac{G_{IC}}{a_C} = \frac{2\pi v \sigma_Y^2}{E} = \varphi \qquad (1)$$

where G_{IC} is the critical ratio of energy release in crack propagation, a_C is the half defect size, σ_Y is the applied stress equal to yield stress, v and E are respectively the Poisson's ratio and the Young's modulus, so that φ is a material's property. The crack propagates if $G_{IC}/a_C < \varphi$ and does not propagate if $G_{IC}/a_C > \varphi$. This relationship is only valid for brittle and elastic materials, but it can be generalized as follows.

According to (1), there are only two ways leading to fracture for a given applied stress: toughness decrease (G_{IC}) or defect size increase (a_C). Both ways can be envisaged in the case of aging: the first one would correspond to homogeneous degradation, G_{IC} being an increasing function of molar mass, i.e. a decreasing function of the number of chain scissions. The second one would correspond to heterogeneous degradation, as evidenced, for instance, from chemiluminescence experiments by Celina and George [9]. In the first case (toughness decrease), use of molar mass–fracture property relationships would have a physical meaning. In the second case, average molar mass or any species concentration values would not be the relevant parameters. Although the coexistence of homogeneous and heterogeneous processes is not excluded, it will be tried here to demonstrate that, for the polymers under consideration, aging-induced embrittlement results from the first way, i.e. the toughness decrease associated to a homogeneous degradation. Two types of arguments will be used: (1) about defect size at the embrittlement point and (2) about the fact that degraded polymers behave in the same way as virgin ones showing a same molar mass value.

Defect size at the embrittlement point

Applications of Eq. 1 to PP or PE, for which G_{IC} typically ranges between 6 and 8 kJ m^{-2} [3], would lead to a_C values of the order of 1 cm, that is, no doubt, excessive. Furthermore, it is well known that visible scratches do not affect significantly the strength of PP injection molded bumpers or PE rotomoulded tanks. In these ductile polymers, it is clear that defects must be relatively large to induce brittleness. However, this conclusion is not consistent with the fact that embrittlement occurs at an extremely low (average) aging conversion, for instance, in PP, before the appearance of a carbonyl peak in IR spectra [1].

In some cases, brown spots could appear during oxidation after an induction period [10]. This indicates the build-up of quasi-isotropic heterogeneities in PP thermal oxidation after the end of induction period. However, the extrapolation of their size to short times seems to indicate that they nucleate after embrittlement time [11]. When available, SAXS measurements do not indicate the

existence of density fluctuations linked to an eventual defect build-up [12]. In the same way, positron annihilation measurements show no change in the size of free volume holes of PP after photo-oxidation [13]. Last but not least, steric exclusion chromatograms of oxidized samples do not reveal the polydispersity increase or, even, the build-up of a low molar mass component attributable to localized degradation. In contrast, progressive shift of molar mass distribution toward low values with a decrease of polydispersity index (when this latter is initially higher than 2), both characteristic of homogeneous random chain scission, is observed in PP photo-oxidation [14, 15], thermal oxidation in solid state [16–19], and probably also in radiochemical oxidation, although in this latter case the polydispersity index values were not reported [20]. Some observations were made in the case of PE thermal oxidation in solid state [21–23], although in some cases, anomalous stabilizer depletion could explain some anomalous behavior in stabilized samples [21]. Viebke et al. [21] mentioned that polybutene-1 behaves in the same way as PE. Photo-oxidation [24] and radio-oxidation [25] of PE led to similar observations. However, crosslinking can compete with chain scissions in PE oxidation, which can lead to a polydispersity increase, as it has been found by Fayolle et al. [26] by studying molar mass distribution of thermally oxidized metallocene-PE samples. But in all cases, M_W decreases as soon as the exposure begins, which indicates clearly the existence of a homogeneous degradation process. Molar mass data are also available for POM thermal oxidation at 130 °C [27]: they indicate clearly the existence of homogeneous degradation.

These observations can appear surprising since it is well known that oxidation is heterogeneous at the morphological scale: it occurs only in the amorphous phase because molecular reagents (oxygen, water…) are insoluble in the crystalline phase. This latter is organized in more or less regularly spaced lamellae with long periods typically few dozens of nanometers. There is a wide consensus (see below) on the fact that ductility is linked to the presence of macromolecules of which the gyration radius is higher than the long period, which allows the existence of tie-chains interconnecting lamellae. Two possible distributions of chain scission events can be distinguished. They are schematized in Fig. 1.

In the case (a) where scissions are homogeneously distributed in the amorphous phase, degradation will display the characteristics of a random chain scission at low conversions. At relatively high conversions, however, the molar mass distribution will display regularly spaced peaks corresponding to a small integer number of crystalline segments (Fig. 1c) [11].

"Critical" molar mass for ductile–brittle transition in virgin and degraded polymers

The most common parameter used to characterize the ductile–brittle transition in the polymer under study is the ultimate strain ε_R or the ultimate draw ratio $\lambda_R = 1 + \varepsilon_R$.

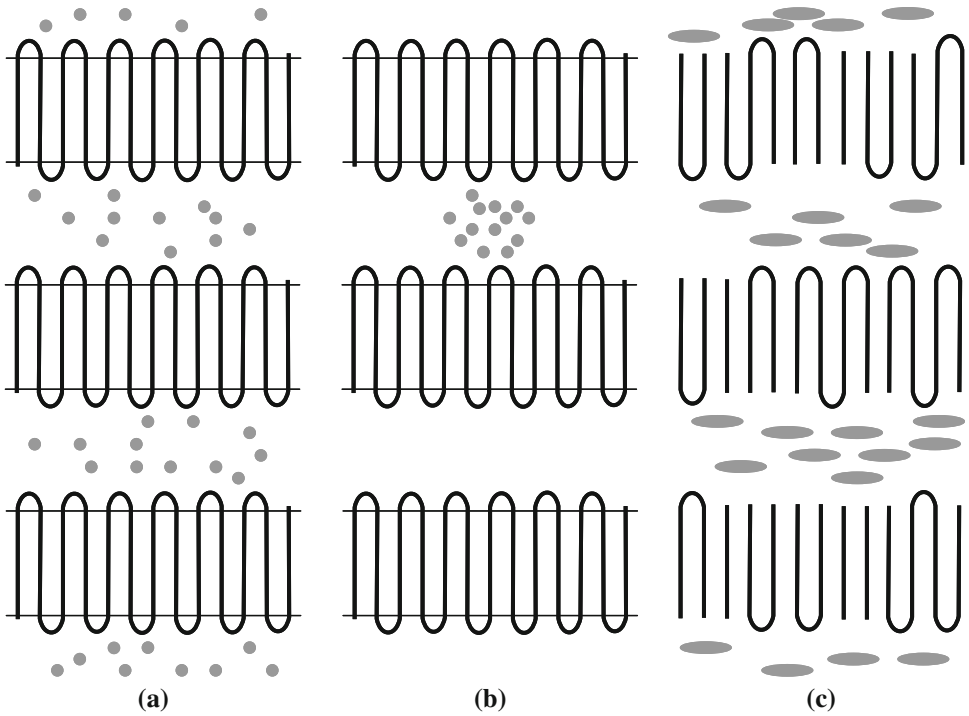

Fig. 1 Schematization of two possible distributions of scission events at the lamellae scale (**a**, **b**), and highly degraded state (**c**)

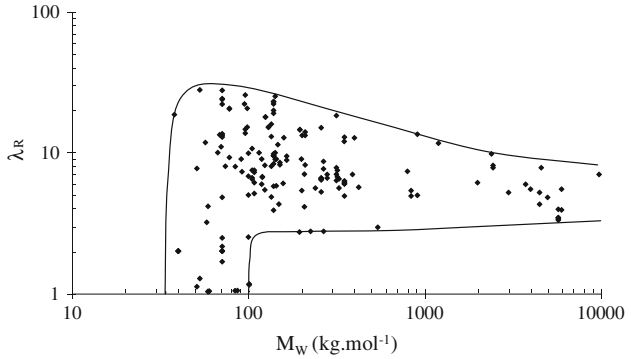

Fig. 2 Ultimate draw ratio determined from tensile testing (λ_R) versus weight average molar mass (M_W) from literature data [26]

Its change with molar mass M_W displays generally the shape of Fig. 2.

Brittle and ductile regimes of rupture can be well distinguished by the absence in the former and the presence in the latter of a plastic deformation. In the ductile regime, λ_R is a slowly decreasing function of M_W, attributed to the increase of entanglement density. The ductile–brittle transition occurs in a more or less sharp molar mass interval. In a first approach, it will be considered that it corresponds to a critical molar mass M'_C (M_C being the critical rheological mass, $M'_C \geq M_C$ in all cases). In the case of PE, the graph $\lambda_R = f(M_W)$ has been built from compiled literature data irrespective of the polymer microstructure, processing conditions, strain rate, aging history [26]. This graph displays the shape of Fig. 2, the ductile–brittle transition being spread over the 40–100 kg mol^{-1} molar mass interval. One can conclude for the time being that $M'_C = 70 \pm 30$ kg mol^{-1}. In this set of data, virgin samples cannot be distinguished from degraded ones.

The same analysis can be made for PP. For virgin samples, the ductile–brittle transition is always located between 170 and 250 kg mol^{-1} [19, 28–30]. Concerning degraded samples, it has been found that $M'_C = 200$ kg mol^{-1} in the case of photo-oxidation [31] and thermal oxidation [1], and 180 kg mol^{-1} in the case of radiochemical oxidation [20].

From this short review, it is clear that if systematic differences exist between degraded and virgin samples of same average molar mass, they are too subtle to be observed in such compilations, owing to the multiple sources of scatter, especially those relative to molar mass measurements.

It can be concluded that, in the polymers under investigation, molecular weight data indicate that there is always a homogeneous random chain scission process, which does not exclude the coexistence of a heterogeneous one, and that embrittlement is due to the decrease of molar mass resulting from the homogeneous process. Embrittlement is linked consequently to a decrease of polymer toughness rather than from defects build-up. As a result, molar mass can be considered as the key parameter to characterize aging effects in the cases under study.

Why embrittlement occurs at so high molar mass?

Let us compare, in Table 1, three amorphous glassy polymers and three semi-crystalline polymers having their amorphous phase in rubbery state [1, 3, 26, 27, 32–35].

For a polymer of number average molar mass M_{N0}, the concentration v_0 of entanglement strands is given by:

$$v_0 = \frac{1}{M_E}\left(1 - \frac{2M_E}{M_{N0}}\right) \tag{2}$$

with M_E being the molar mass between entanglements for the given polymer.

At the embrittlement point, the number of broken entanglement strands is given by:

$$s_C = 2\left(\frac{1}{M'_C} - \frac{1}{M_{W0}}\right) = \frac{2}{M'_C}\left(1 - \frac{M'_C}{M_{W0}}\right) \tag{3}$$

The fraction of broken entanglement strands at the ductile–brittle transition is therefore:

$$\frac{s_C}{v_0} = \frac{2M_E}{M'_C}\left[\frac{1 - \frac{M'_C}{M_{W0}}}{1 - \frac{2IP_0 \times M_E}{M_{W0}}}\right] \tag{4}$$

where IP_0 is the initial polydispersity index. For high initial molar masses:

Table 1 Critical molar mass for ductile–brittle transition (weight average) (M'_C), entanglement molar mass (M_E), and ratio M'_C/M_E for three glassy polymers and semi-crystalline polymers

Polymer	Acronym	M'_C (kg mol^{-1})	Reference	M_E (kg mol^{-1})	Reference	M'_C/M_E
Poly(bisphenol A carbonate)	PC	28	[33]	1.78	[32]	16
Poly(methyl methacrylate)	PMMA	40	[3]	9.2	[32]	4
Polystyrene	PS	60	[32]	18.7	[32]	3
Polyethylene	PE	70	[26]	1.4	[32]	50
Polypropylene	PP	200	[1]	3.5	[33]	57
Polyoxymethylene	POM	70	[60]	2.5	[32]	28

$$\frac{s_C}{v_0} = \frac{2M_E}{M'_C} \quad (5)$$

One sees that, in amorphous polymers of Table 1:

$$\frac{s_C}{v_0} > 12\%$$

whereas for semi-crystalline polymers having their amorphous phase in rubbery state:

$$\frac{s_C}{v_0} < 7\%$$

In other words, in this latter polymer family, ductile–brittle transition occurs before the entanglement network has been significantly damaged, whereas in amorphous polymers, the destruction of the entanglement network can be reasonably considered as the direct cause of embrittlement.

There are two possible ways to explain the fact that $M'_C \gg M_E$. The first one is that the lamellar morphology determines a critical chain dimension not related to the entanglement molar mass, but longer than this latter. Two important quantities have to be considered in this case: the lamella thickness l_c and the long period l_p. Some theories trying to establish a link between the lamellar structure and the critical molar mass have been recently reviewed by Plummer [36]. For instance, for Tervoort et al. [37] one could have:

$$M'_C \sim 3M_L$$

where M_L is the molar mass of the chain segment corresponding to lamella thickness. For PE, $M_L \sim$ 10–14 kg mol^{-1}, which leads to a M'_C value significantly lower than the experimental value: $3M_L \sim$ 30–40 kg mol^{-1} against 40–100 kg mol^{-1} experimental values. For Benkonski et al. [38], the onset of ductility would be reached for chains having their end-to-end distance of the order of the long period l_p, which would lead to:

$$M'_C = \frac{l_p^2 M_m}{C_\infty l^2} \quad (6)$$

where M_m is the molar mass of an elementary chain unit of which the length is l and C_∞ is the chain characteristic ratio. In PE, for example, $C_\infty = 6.8$ and $l = 0.154$ nm. The long period is an increasing function of the molar mass which can vary between 15 and 40 nm in PE. The lowest value of M'_C would be thus close to 20 kg mol^{-1}, a value significantly lower than the experimental one.

The l_p value corresponding to $M'_C = 70$ kg mol^{-1} is 28 nm. In reality, such long periods are found in PE samples of M_W higher than 200 kg mol^{-1}.

Many authors tried to interpret aging-induced embrittlement in terms of tie-molecules interconnecting lamellae. Embrittlement would correspond to a critical tie-molecules concentration. The problem here is that embrittlement occurs when a relatively small fraction of chain has been broken.

Some authors, for example Oswald and Turi [39] in the case of PP thermal oxidation, suggested that oxidation attacks selectively tie-chains. On the other hand, we know that tie-chains constitute only a relatively small fraction of the whole number of chains [40]. How to explain the selectivity of oxidation? The second and promising way of explanation of the fact that embrittlement occurs at very high molar mass in the polymer family under consideration is that chain scission induces morphological changes. The true critical quantity would be therefore a morphological parameter rather than a molar mass. The following sections are aimed to explore this way.

Does random chain scission modify crystallinity?

Molar mass changes

Let us recall that molar mass distribution can be modified by random chain scission or crosslinking. The average molar masses are linked to the number s of chain scission and x of crosslinking events (per mass unit) by Saito's equations [41]:

$$\frac{1}{M_N} - \frac{1}{M_{N0}} = s - x \quad (7)$$

$$\frac{1}{M_W} - \frac{1}{M_{W0}} = \frac{s}{2} - 2x \quad (8)$$

In the following, only "pure" random chain scission will be considered ($x = 0$). The above equations lead then to the following expression for M_W and for the polydispersity index I:

$$M_W = \frac{M_{W0}}{1 + s \times \frac{M_{W0}}{2}} = \frac{M_{W0}}{1 + \frac{C}{2}} \quad (9)$$

$$I = I_0 \times \frac{1 + \frac{C}{I_0}}{1 + \frac{C}{2}} \quad (10)$$

where $C = s \times M_{W0}$ is the number of chain scission events per initial weight average chain. Equation 10 shows that I increases when $I_0 < 2$ and decreases when $I_0 > 2$ but tends toward 2 in both cases.

Indeed, both average molar mass values, M_N or M_W, can be, in principle, indifferently chosen to express degradation effects since they are interrelated. Here, however, M_W will be preferred, first because it is easier to determine, for instance from rheometric data, second because fracture properties seem to be governed mainly by M_W as shown by the example of tensile ultimate elongation for HDPE [42–46]. In a detailed study of crystalline morphology–molar mass relationships, Robelin-Souffaché and Rault [47] find

that the key parameter is the weight average gyration radius that leads to consider a new average molar mass, M_R, defined by:

$$M_R^{1/2} = \sum_i \left(\frac{N_i M_i}{\sum_i N_i M_i} \right) M_i^{1/2} \quad (11)$$

where M_R is intermediary between M_N and M_W but closer to M_W so that it will be considered that, at least in a coarse grain approach, M_W is a pertinent quantity.

Effect on chain scission on crystallinity ratio

In quenched semi-crystalline polymers, crystallization is limited by the presence of chain entanglements in the melt [47]. Chain scissions occur in the amorphous phase and liberate chain segments, which will integrate the crystalline phase if they have sufficient mobility, which is the case in rubbery state. This process, called chemicrystallization, was observed one half century ago in PET hydrolysis [48] and in polyolefins oxidation [49–51]. In the following decades, results showing the existence of chemicrystallization were accumulated as shown by the non-exhaustive compilation summarized by Table 2 [52–70].

Crosslinking tends to inhibit crystallization. This is clearly put in evidence in case of gamma-irradiated PE where oxidative chain scission predominates in a superficial layer (because oxidation is diffusion controlled) whereas anaerobic crosslinking predominates in the core [70].

Quantitative studies of chemicrystallization are often complicated by the following processes:

1. The loss of small molecules by evaporation (in the case of oxidation) or extraction by water (in the case of hydrolysis). Since the loss exclusively comes from amorphous phase degradation, it contributes to an increase of crystallinity ratio.
2. In the case of hydrocarbon polymer oxidation, there is a density increase due to the incorporation of "heavy" oxygen atoms to the chains. The density can largely overtake the value ρ_c corresponding to 100% of crystallinity, as shown for instance for crosslinked PE [71].
3. In the case of irradiation by ionizing radiations, radiochemical events occurring into the crystalline phase induce a decrease of crystallinity ratio which can compensate, at least partially, the effect of chemicrystallization. In well oxygenated regions, however, the radiochemical yield of crystal destruction is low compared to the crystallization yield, so that crystallization is easily observable.
4. In the case of thermal aging, annealing effects can coexist with chemicrystallization ones when the samples are initially undercrystallized. The amplitude of annealing effects can be easily appreciated by comparing degraded samples with samples having undergone the same thermal treatment but with the absence of the degrading agent (oxygen in the case of thermal aging, water in the case of hydrolysis [54]).

Fortunately, crystallinity changes become often observable at low conversion of the degradation process, when all the above-mentioned problems, except indeed (4), are negligible. This means that chemicrystallization is characterized by a relatively high yield. The latter can be defined as the number y of monomer (or elementary chain segment) units entering in the crystalline phase per scission event.

The instantaneous value $y(t)$ of this yield is given by:

$$y(t) = \frac{1}{M_m} \times \frac{dx_c}{dt} \Big/ \frac{ds}{dt} \quad (12)$$

where M_m is the molar mass of the monomer unit, x_c is the crystallinity ratio, and s is the number of chain scission event per mass unit.

Quantitative data on chemicrystallization are relatively scarce in the literature: In the case of PET hydrolysis at 100 °C, Ballara and Verdu [54] reported a value of 5–6 monomer units per scission. In the case of thermal PE thermal oxidation in the 70–105 °C temperature range, Viebke et al. [21] found a value of 45 methylenes per scission. About the same value was found by Fayolle et al. [27] in the POM thermal oxidation at 130 °C. These values can be compared with the length of entanglement strands in the melt, in Table 3.

It can be seen that, in all cases, the length of the chain segments entering the crystalline phase after one chain scission is an important fraction of the entanglement strand, often ~50% or more. Is it possible to derive this result from structure–property relationships established on virgin

Table 2 Literature references about chemicrystallization

Degradation mode	PET	PP	PE	POM
Thermal oxidation in solid state	–	[39, 55–58]	[59]	[60]
Photochemical oxidation	–	[61, 62]	[66–68]	–
Radiochemical oxidation	–	[63, 65]	[70]	–
Hydrolysis	[52–54]	–	–	–

Table 3 Entanglement molar mass (M_E) [34, 35], number of monomer units per entanglement strands (N_E), chemicrystallization yield $y(t)$, and ratio $y(t)/N_E$

Polymer	M_E (g mol^{-1})	N_E	$y(t)$	$y(t)/N_E$
PE	1390	100	45	0.45
POM	2590	85	40–50	0.47–0.59
PET	1450	7.5	5–6	0.67–0.80

polymer samples? From a theoretical analysis, Robelin-Souffaché and Rault [47] proposed:

$$x_c = 1 - \psi\left(\frac{1}{r_{WE}} - \frac{1}{r_W}\right) \quad (13)$$

where r_W and r_{WE} are the weight average gyration radii for respectively the polymer under consideration and a polymer of which the molar mass is close to the entanglement threshold. ψ is a parameter depending on chemical structure and crystallization conditions.

Considering that, in a first approximation:

$$r_W \propto M_W^{1/2} \quad (14)$$

Equation 13 becomes:

$$x_c = a + b \cdot M_W^{-1/2} \quad (15)$$

where a and b depend on the chemical structure and crystallization conditions.

It has been tried to check Eq. 15 in the case of HDPE with available data [42, 72–74] plotting x_c against $M_W^{-1/2}$ (Fig. 3).

Although the results are relatively scattered, a linear dependence can be assumed. The parameters a and b of the straightline and correlation coefficient R^2 are given in Table 4. These data call for the following comments: These results are too scattered to be considered as good proofs of validity of the Robelin-Souffaché and Rault's theory [47], but this is not very surprising since we know that crystallinity depends on precise cooling conditions and thermal history in molten state prior to crystallization [47]. Furthermore, due to the approximation made in Eq. 14 (M_R assimilated to M_W), the parameters must display some dependence with polydispersity. These scattering sources must be added to experimental ones, as well on x_c as on M_W measurements. According to the starting theory (Eq. 13), all the straightlines $x_c = f(M_W^{-1/2})$ must converge on a point of coordinates $x_c = 1$, $M_W = M_{WE}$. M_{WE}, the "entanglement threshold molar mass", is given by:

$$M_{WE} = \left(\frac{b}{1-a}\right)^2 \quad (16)$$

The values of M_{WE} calculated from Eq. 16 are listed in Table 4. The series of isothermally crystallized samples from Kennedy et al. [42] has been put apart because no dependence of x_c with M_W was found. M_{WE} values range between 1100 and 6400 g mol^{-1}, which is the good order of magnitude, considering that the entanglement molar mass is close to 1400 g mol^{-1} and that M_{WE} can be significantly higher owing to polydispersity effects. The results of Fig. 3 and Table 4 clearly show that the relationship between M_W and x_c cannot be described by a single curve, which is not very favorable to the project of including chemicrystallization into a kinetic model. A possibility would remain, however, if one assumes that the Robelin-Souffraché and Rault's law [47] applies to a sample undergoing degradation. In this case, all the points ($M_W^{-1/2}$, x_c) corresponding to distinct aging times would be located in a straightline of which two points are known: the departure point ($M_{W0}^{-1/2}$, x_{c0}) and the point corresponding to entanglement threshold ($M_{WE}^{-1/2}$, 1). The equation of the straightline can be then determined. By using Eqs. 15 and 16, the relationship between x_c and M_W can be expressed as:

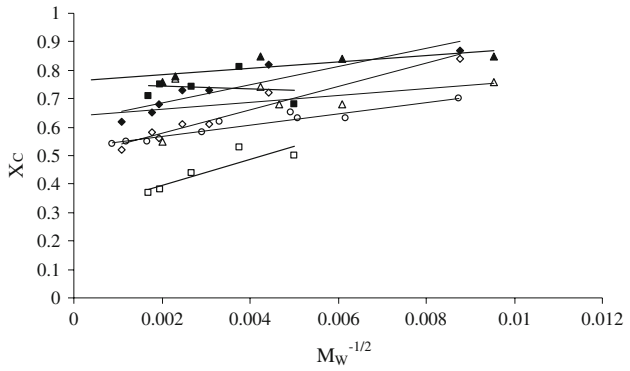

Fig. 3 Crystallinity ratio (x_C) versus $M_W^{-1/2}$ for quenched (*open symbols*) and isothermally crystallized (*closed symbols*) HDPE samples. ■, □: from Kennedy et al. [42]; ◯: from Nitta and Tanaka [72]; ▲, △: from Voigt-Martin and Mandelkern [73]; ◆, ◇: from Jordens et al. [74]

Table 4 Parameters of Eq. 15, coefficient of correlation for the linear regression, and entanglement threshold molar mass calculated from Eq. 15

Authors	Reference	Crystallization conditions	a	b (mol$^{1/2}$ g$^{1/2}$)	R^2	$(b/1-a)^2$ (g mol^{-1})
Voigt-Martin and Mandelkern	[73]	Q	0.6364	12.548	0.181	1191
	[73]	IC	0.7634	10.89	0.623	2118
Kennedy, Peacock, and Mandelkern	[42]	Q	0.3058	45.795	0.776	4352
	[42]	IC	0.7535	5.121	0.0206	–
Nitta and Tanaka	[72]	Q	0.5281	19.994	0.9191	1795
Jordens, Wilkes, Janzen, Rohlfing, and Welch	[74]	IC	0.53	35	–	5545
	[74]	Q	0.5	40	–	6400

Q quenched samples, *IC* isothermally crystallized samples

$$x_c = x_{c0} + \frac{1 - x_{c0}}{\left[\left(\frac{M_{W0}}{M_{WE}}\right)^{1/2} - 1\right]}\left[\left(\frac{M_{W0}}{M_W}\right)^{1/2} - 1\right] \quad (17)$$

where

$$\frac{M_{W0}}{M_W} = \left(1 + \frac{C}{2}\right) \quad (18)$$

In the range of interest ($0.5 \leq C \leq 10$), calculation proves that the expression between brackets of Eq. 17 can be approximated by:

$$\left(1 + \frac{C}{2}\right)^{1/2} - 1 \approx C/5 \quad (19)$$

So that:

$$x_c = x_{c0} + BC \quad (20)$$

where

$$B = \frac{1}{5}\frac{1 - x_{c0}}{\left[\left(\frac{M_{W0}}{M_{WE}}\right)^{1/2} - 1\right]} \quad (21)$$

The crystallization yield is:

$$y = \frac{1}{M_m}\frac{dx_c}{ds} = \frac{1}{M_m}\frac{dx_c}{dC}\frac{dC}{ds} \quad (22)$$

It comes:

$$y = B\frac{M_{W0}}{M_m} \quad (23)$$

where M_m is the molar mass of the monomer unit or the elementary chain unit (methylene in the case of PE). A numerical application has been made in three cases: PE thermal oxidation with characteristics close to the ones studied by Viebke et al. [21], POM thermal oxidation with characteristics close to the ones studied by Fayolle et al. [27], and PET hydrolysis in conditions close to the ones studied by Ballara and Verdu [54]. The results are reported in Table 5. They call for the following comments:

1. Equation 23 predicts good order of magnitude for the chemicrystallization yield in POM and PET.
2. For PE, the calculated value is about three times higher than the experimental one. In fact, Viebke's result was obtained for a copolymer grade for pipe extrusion in which branching limits crystallization. Our calculation was made for linear PE in which the crystallization yield must be, indeed, higher.

To conclude this section, Eq. 17 or its simplified version Eq. 23 valid at low conversions of the degradation process seems to be an interesting way to predict the chemicrystallization yield, because it is based on reasonable hypotheses, contains no adjustable parameters, and is very simple. However, its validity is limited to linear homopolymers. The chemicrystallization yield appears to be proportional to the initial amorphous content ($1 - x_{c0}$) and to the initial weight average degree of polymerization M_W/M_m. It is also a slowly increasing function of the entanglement molar mass.

The relatively good predictive value of Eq. 23 can appear surprising considering the multiple sources of scatter. It can be understood, at least in the case of thermal aging, because aging imposes a long duration thermal treatment during which the polymer can reach a quasi-equilibrium mainly determined by molar mass distribution and the initial morphology. From a practical point of view, however, consideration of x_c rather than M_W will not improve the accuracy of a kinetic model based on the above equations. Furthermore, as it will be seen next, the concept of critical crystallinity ratio corresponding to ductile–brittle transition would be questionable: for a given x_c value, it is possible to observe both mechanical behaviors.

Effect of chain scission on lamellar structure

There is now a wide consensus on the fact that fracture properties are mainly governed by the lamellar morphology [36, 75–77]. Although the lamella length, or better, its aspect ratio, plays a non-negligible role, at least in elastic properties [78], it is usual to focus on transverse dimensions of lamellae stacks, i.e. the long period l_p, the lamella thickness l_C, and the thickness of the amorphous layer separating two adjacent lamellae l_a. These quantities are interrelated as follows:

$$l_p = l_c + l_a \quad (24)$$

$$l_c = x_c\frac{l_p\rho_a}{\rho_c - x_c(\rho_c - \rho_a)} \quad (25)$$

where ρ_c and ρ_a are the densities of crystalline and amorphous phase respectively. l_p can be determined by

Table 5 Calculated (according to Eq. 22) and experimental chemicrystallization yields, M_{WE} being assimilated to the entanglement molar mass M_E

Polymer	M_{W0} (kg mol^{-1})	M_{WE} (kg mol^{-1})	M_m (kg mol^{-1})	$B \times 10^3$	y_{calc}	y_{exp}	Reference
PE	200	1.4	0.014	9.5	136	45	[20]
POM	140	2.5	0.03	16.0	75	45–50	[60]
PET	40	1.5	0.192	25.0	5	5–6	[54]

SAXS [47], l_c can be determined by Raman spectroscopy [79] or from melting point T_M using Gibbs–Thomson equation:

$$l_c = \frac{2\sigma}{\rho_c \Delta H_M} \frac{T_{M0}}{T_{M0} - T_M} \quad (26)$$

where σ is the surface energy, T_{M0} is the equilibrium melting point, and ΔH_M is the melting enthalpy of crystal.

As noticed by Gedde and Ifwarson [80], the parameters of this equation, especially σ and ΔH_M, can vary during oxidative aging so that this approach for estimating l_c can be used with caution. At least, l_p, l_c, and l_a can also be determined from micrographs obtained by electron microscopy when well resolved images are available [36, 73, 76].

Schematically, for virgin samples, l_c appears almost independent of molar mass whereas l_a is an increasing function of molar mass. l_c depends sharply on the crystallization temperature, it is almost proportional to the reciprocal of supercooling. In some polymers, however, l_c increases with M_W. For instance, for HDPE quenched samples. Nitta and Tanaka [72] find that l_c increases from about 10 nm at $M_W \sim 10$ kg mol^{-1} to about 20 nm at $M_W = 1000$ kg mol^{-1}. The same trend was observed by Kennedy et al. [42]. All the authors find that l_a is an increasing function of M_W [42, 47, 72, 73, 77] as shown by Fig. 4 where l_a appears to be a linear function of the square root of M_W:

$$l_a = 3.67 + 0.015 \times M_W^{1/2} \quad (27)$$

l_a being expressed in nanometers and M_W in g mol^{-1}.

Robelin-Souffaché and Rault [47] found:

$$l_a = 1.2 + 0.044 \times M_R^{1/2} \quad (28)$$

This equation cannot be valid in the whole full range of M_W values, otherwise it would disagree with Eq. 13 according to which $x_c = 1$, i.e. $l_a = 0$ at a molar mass close to the entanglement threshold. It will be supposed, here, that it remains valid in the molar mass domain of interest, relatively far above the entanglement threshold.

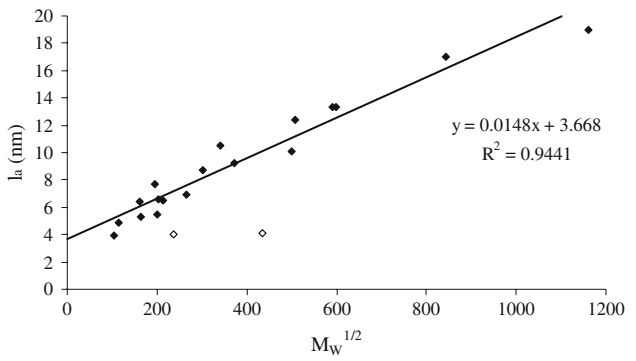

Fig. 4 Interlamellar spacing l_a versus square root of the weight average molar mass. Compilation of literature data (see text). ◇: apparently aberrant points eliminated for the review

Since $M_W/M_R > 1$, the difference of slopes in Eqs. 26 and 27 is not very surprising. According to Nitta and Tanaka [70], l_a would be independent of the comonomer content in ethylene co hexene 1 copolymers, which could simplify the study of these materials, for instance in studies of PE for pipe extrusion [77].

Data relative to the aging effects on lamellar morphology are relatively scarce in the literature. In the case of crosslinked PE, Gedde and Ifwarson [80] studied the changes of melting characteristics during thermal aging and tried to apply the Gibbs–Thompson equation to determine l_c. l_c was found to increase significantly after aging but, as noticed by the authors, this method is complicated by changes of parameters such as the surface energy (which decreases). Zhang and Cameron [13] have performed SAXS and WAXS measurements on gamma-irradiated PP samples. The crystallinity ratio increases slightly: 2–3% for 50 kGy irradiation dose, independently of the initial morphology. The long period is almost constant, whereas l_a decreases slightly but significantly. At high doses, the phenomenon tends to be masked by the effect of crystal destruction due to the occurrence of radiolysis events within crystals, which is not the case in thermo or photo-oxidation. In the case of POM thermal oxidation at 130 °C, Fayolle et al. [60] found also a decrease of l_a after an initial period dominated by annealing effects. Here, the mass loss due to depolymerization can also contribute to the decrease of l_a.

Despite the scarceness of published data about aging effects on lamellar morphology, it seems reasonable to assume the mechanism illustrated by Fig. 5. Chemicrystallization would proceed by lamellae thickening at the expense of the amorphous phase, the long period remaining constant. In polymers such as PE, PP, or POM, chemicrystallization seems to occur exclusively through lamella thickening. In other polymers, especially those having a relatively low crystallinity ratio, chemicrystallization involving the nucleation of new crystals is not excluded. This mechanism is probably the cause of the decrease of long period in polyamides submitted to hydrolysis [81].

To conclude this section, it is well established that chain scission induces an increase of the crystallinity ratio and a decrease of the interlamellar spacing l_a. These morphological changes become significant at low conversion of the degradation process. It remains to determine if these changes can be responsible for embrittlement and which is the most pertinent quantity to use in kinetic modeling.

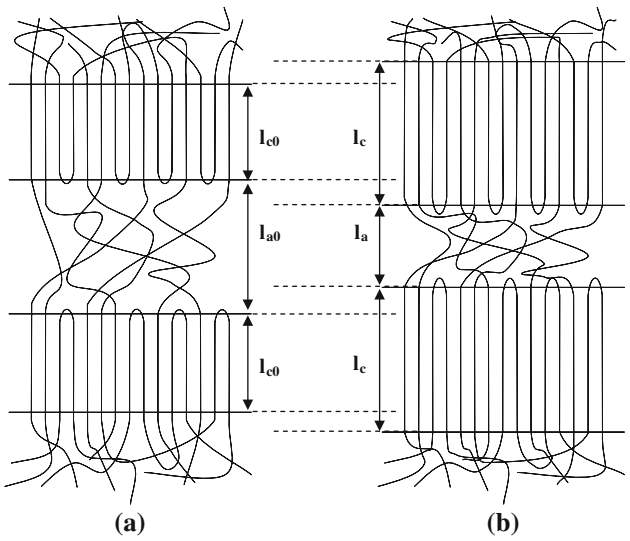

Fig. 5 Hypothetical changes of lamellar dimensions after crystallization: **a** initial sample and **b** aged sample

How to choose an embrittlement criterion?

The embrittlement mechanism is not clearly elucidated so that the embrittlement criterion cannot theoretically be deduced from this mechanism. Schematically, two main ways of explanation seem possible:

1. A molecular interpretation in which, for instance, the entanglement density or the tie-macromolecule concentration would be the key quantities.
2. A micromechanical interpretation in which lamellar dimensions would play the key role through stress concentration effect, control of cavity radius in cavitation processes [75] or simply from the fact that small amorphous domains cannot sustain large deformations [42].

Concerning the nature of the embrittlement criterion, it could be "single", e.g. a critical value of a given property: crystallinity ratio, molar mass, etc., or "composite", e.g. a boundary in a multidimensional space, for instance a curve in the molar mass-crystallinity ratio map, separating "ductile" and "brittle" regions. Some "single" criteria can be set aside in a first approach: molar mass and entanglement density for already seen reasons, or crystallinity ratio despite the existence of favorable arguments [82]. As a matter of fact, for samples of close molar mass, $M_W = 51$ and 54 kg mol^{-1}, it is possible to obtain a ductile or a brittle behavior depending on thermal treatments, but the ductile–brittle transition was located at $x_c = 0.62$ by Voigt Martin et al. [73] and $0.70 \leq x_c \leq 0.78$ by Jordens et al. [74]. Such differences, as well as the scatter observed in x_c–M_W relationships, indicate that if the overall crystallinity ratio (or amorphous phase content) is a pertinent quantity, it cannot be established from a compilation of literature data. Anyhow, there are many reasons to suppose that the fracture behavior depends rather on factors such as the lamellar dimensions or the tie-macromolecule concentration.

Table 6 Lamellar dimensions for two HDPE samples isothermally crystallized (C) or quenched (Q) [73]

M_W (kg mol^{-1})	Thermal treatment	l_p (Å)	l_c (Å)	l_a (Å)
250	C	460	332	128
250	Q	207	106	101
5.6	C	255	208	47
5.6	Q	135	95	40

First, concerning the lamellar dimensions, one can expect the same data scatter for the long period l_p or the lamella thickness l_c as for the crystallinity ratio, because they sharply depend on thermal history. In contrast, the interlamellar spacing l_a appears to be less dependant on thermal history, as illustrated for instance, by the data of Table 6 from Voigt-Martin and Mandelkern [73].

It is clear that l_a varies considerably less than l_p or l_c with the crystallization conditions but is sharply linked to molar mass (Fig. 4). In their extensive study of tensile properties of HDPE, Kennedy et al. [42] have compared samples differing by their molar mass distribution and their crystallization conditions. They put in evidence the fact that the ductile–brittle transition occurs always when the interlamellar spacing reaches a critical value: $l_a = l_{aC} = 6$–7 nm. A recent study on POM thermal oxidation led to a similar observation, with a close value for l_{aC} [60].

These results militate in favor of the choice of interlamellar spacing as "single" criterion for ductile–brittle transition. According to Eq. 27, l_a values of 6 and 7 nm would respectively correspond to 24 and 49 kg mol^{-1}. Is it possible to reach a better precision?

Tie-macromolecules

As soon as the concept of tie-macromolecule appeared [83], there were authors to attribute embrittlement to their scission [39]. This interpretation reappeared then regularly in the literature, for instance to explain embrittlement of PP submitted to radiochemical aging [63, 64]. The problem is that, especially in PP, embrittlement occurs when a very small fraction of chains has been broken [40]. Indeed, random chain scission occurs preferentially on the longest chains, i.e. on the fraction of chains able to establish interlamellar links. Tie chains have thus a higher probability to be broken than "average chains" but is this probability high enough to compensate the scarceness of

chain scission events? The problem here is to translate this question into quantitative relationships.

In his extensive critical review, Seguela [84] has compared the experimental and theoretical approaches of the tie-macromolecule concentration. No one has applied these approaches to the study of aging-induced embrittlement to our knowledge. For instance, the experimental method of Kriegbaum et al. [85] based on analysis of strain hardening during plastic flow, using rubber elasticity concepts to determine the concentration of mechanically active chains, seems interesting because there is an impressive number of aging studies reporting tensile curves, e.g. allowing in principle to quantify strain hardening. Unfortunately, only engineering tensile curves are reported in these studies, making thus this analysis impossible.

Among theoretical analyses, the one proposed by Huang and Brown [86] with the improvements proposed by Seguela [84] appears especially interesting. According to the basic theory, the probability p of a given chain to become a tie-macromolecule would be given by:

$$p = \frac{1}{3}\frac{\int_L^\infty r^2 \exp\left(-\frac{3}{2}\frac{r^2}{\langle r_0^2\rangle}\right)\mathrm{d}r}{\int_0^\infty r^2 \exp\left(-\frac{3}{2}\frac{r^2}{\langle r_0^2\rangle}\right)\mathrm{d}r} \tag{29}$$

where r_0 is the end-to-end distance and L is given by:

$$L = 2l_c + l_a = 2l_p - l_a \tag{30}$$

In principle, this approach must be applied to every macromolecule of the distribution. Here, it will be assumed, in a first approach, that Eq. 29 applied to the weight average chain gives a good order of magnitude for p. In this case, one can use:

$$\langle r_0^2\rangle = \alpha M_W \tag{31}$$

where α is characteristic of the chemical structure, for instance: $\alpha = 1.42$ Å mol g^{-1} for PE and $\alpha = 0.694$ Å mol g^{-1} for PP.

In case of aging, Eq. 31 can be transformed by substituting M_W by Eq. 9 into:

$$\langle r_0^2\rangle = \frac{\alpha M_{W0}}{1+\frac{C}{2}} \tag{32}$$

If, as suggested above, l_p remains constant during chemicrystallization, Eqs. 27 and 29 give:

$$L = L_0 - 0.015 M_{W0}^{1/2}\frac{1}{\left(1+\frac{C}{2}\right)^{1/2}} \tag{33}$$

where

$$L_0 = 2l_p - 3.67 \quad \text{(in min)} \tag{34}$$

It is then possible to express all the parameters of Eq. 29 in function of the number of chain scissions per initial weight average macromolecule. Indeed, the limit L of integration varies with the crystallization conditions through l_p. We have compared p values in three cases, using data obtained by Nitta and Tanaka [72] on quenched linear PE samples. The results are shown in Fig. 6. The sample characteristics interpolated for two p values, 0.05 and 0.03, have been reported in Table 7.

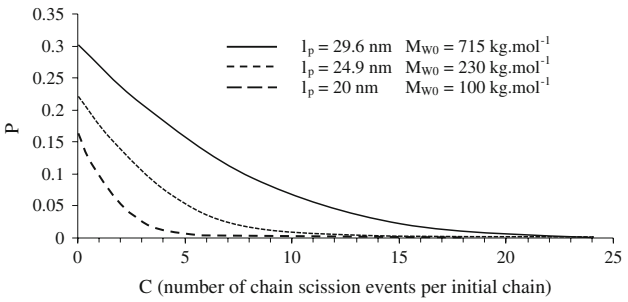

Fig. 6 Probability for a given macromolecule to be a tie-macromolecule (P) versus number of chain scissions per initial weight average chain (C) for three quenched linear PE samples (see text)

The 100–715 kg mol^{-1} molar mass range covers most of the usual PE grades displaying initially a ductile behavior except ultra high molar weight ones. p_F values have been chosen in order to have M_{WF} values coinciding with experimentally found ones, i.e. 40 kg mol^{-1} $\leq M_{WF} \leq$ 100 kg mol^{-1}. As hypothesized, the long period remains constant during degradation, whereas the interlamellar spacing decreases to reach a value l_{aF} at $p = p_F$. l_{aF} tends to increase slightly with the initial molar mass but this dependence could be drawn into the experimental scatter in most of the cases. The corresponding crystallinity ratio x_{cF} has been calculated from $l_{cF} = l_p - l_{aF}$ using Eq. 25, which can be translated into:

$$x_{cF} = \frac{\varphi}{1+\varphi} \tag{35}$$

where

$$\varphi = \frac{l_{cF}\rho_c}{l_{aF}\rho_a} \tag{36}$$

Here, also, a slight dependence of x_{cF} with M_{W0} is expected but it would be observable only in very careful experiments.

Discussion

At this state of our knowledge, we can envisage the use of a "single" embrittlement criterion, e.g. a critical value of the interlamellar spacing, $l_a = l_{aF}$, or "composite" criterion, e.g. a critical value of the tie-macromolecule probability $p = p_F$ which corresponds to a boundary in (l_a, M_W) space. At first sight, there is no way to decide between both

Table 7 Molar mass, interlamellar spacing and crystallinity ratio for $p = 0.05$ and $p = 0.03$, using Eqs. 30–36 for three quenched linear PE samples having the initial characteristics reported by Nitta and Tanaka [72]

M_{W0} (kg mol^{-1})	l_p (nm)	M_{WF} (kg mol^{-1})		l_{aF} (nm)		x_{cF}	
		For $p_F = 0.05$	For $p_F = 0.03$	For $p_F = 0.05$	For $p_F = 0.03$	For $p_F = 0.05$	For $p_F = 0.03$
715	29.6	102	80	8.5	7.9	0.75	0.76
230	24.9	71	58	7.7	7.9	0.72	0.74
100	20.0	50	40	7.0	6.7	0.69	0.70

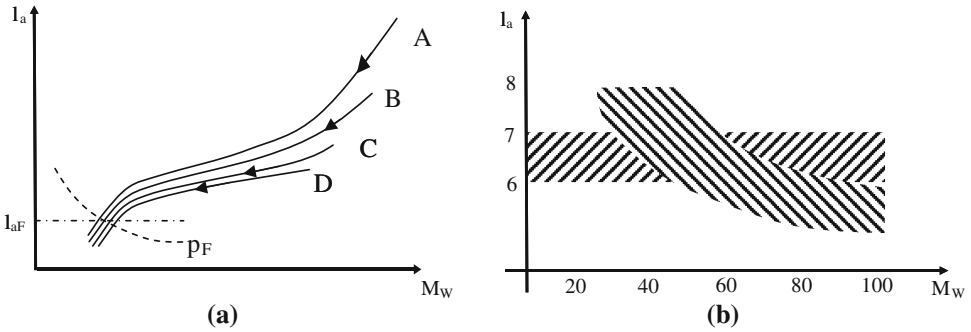

Fig. 7 **a** Schematic representation of ageing trajectories in the (l_a, M_W) map for four samples of which the initial characteristics are the coordinates of the points A, B, C, and D. Two embrittlement criteria are represented: (-·-·-·-) $l_a = l_{aF}$; (- - - -) $p = p_F$. **b** Zoom of the critical zone for HDPE with representation of both embrittlement criteria taking $p_F = 0.03$ for the critical tie-macromolecule probability

criteria, owing to the scatter of available experimental data. The problem can be illustrated by the scheme of Fig. 7 representing aging trajectories in (l_a, M_W) map.

All the aging trajectories are expected to converge in a more or less sharp bottleneck, eventually a single curve if l_a depends only on M_W. The embrittlement criterion will be a horizontal straightline $l_a = l_{aF}$ if the critical property is the interlamellar spacing and a curve corresponding to $p = p_F$ if the critical property is a tie-macromolecule concentration. The example of HDPE (Fig. 7b) shows the difficulty to decide between both criteria.

Conclusion

It has been tried to demonstrate in the above review that when a linear polymer undergoes random chain scission aging, its embrittlement results from a decrease of its toughness rather than from defect build-up. In the case of semi-crystalline polymers having their amorphous phase in rubbery state, embrittlement occurs at an especially low conversion of the degradation process, at which the entanglement network in the amorphous phase has undergone only very little damage. Since these polymers undergo chemicrystallization, it has been hypothesized that this latter could occur by three ways: decrease of the whole amorphous content, decrease of interlamellar spacing or destruction of tie-macromolecules. Relatively abundant data are available on the eventual relationships between ductile–brittle transition and the crystallinity ratio, but their high scatter indicates the existence of important underlying parameters. Very scarce data are available on the role of interlamellar spacing l_a but they favor the hypothesis that embrittlement could correspond to a critical value of l_a, for instance $l_a = 6$–7 nm for PE and for POM. No data are available, to our knowledge, on the role of tie-macromolecule concentration, but applications of the theories of Huang and Brown [86], using a tie-macromolecule probability of 0.03–0.05 would lead to results quantitatively compatible with literature data available on HDPE.

At present time, it seems not possible to decide between the causal chains schematized in Fig. 8.

In the case where the interlamellar spacing would be the pertinent quantity, the embrittlement criterion would be a critical value l_{aF} of l_a. But since l_a is strongly linked to M_W, one can use the corresponding value M_{WF} as an embrittlement criterion that simplifies the approach of lifetime prediction.

In the case where the tie-macromolecule concentration would be the pertinent criterion, the theory of Huang and Brown [86], eventually improved by Seguela [84], could be a way to establish a bidimensional embrittlement criterion. However, the presently available experimental data are too scarce and fuzzy to benefit by such refinements.

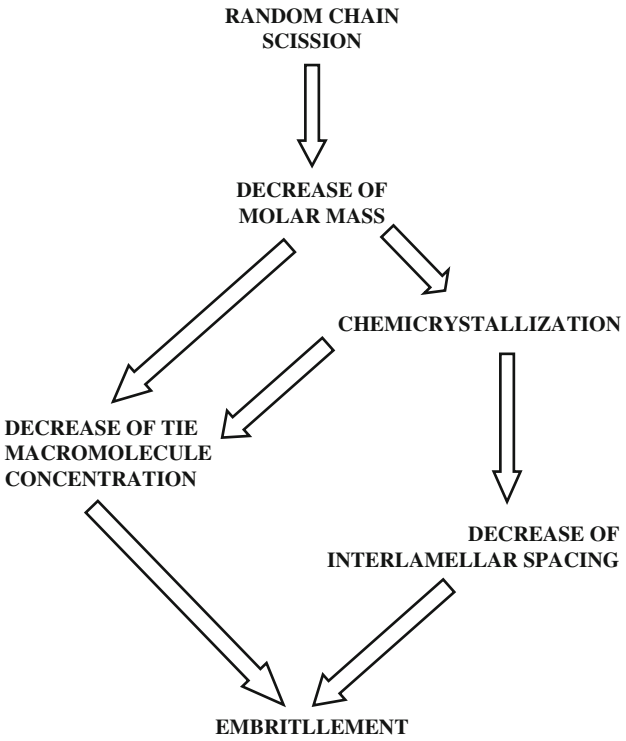

Fig. 8 Schematization of the possible causal chains for degradation-induced embrittlement

References

1. Fayolle B, Audouin L, Verdu J (2000) Polym Degrad Stab 70:333. doi:10.1016/S0141-3910(00)00108-7
2. Brown N, Lu X, Huang YL, Quian R (1991) Macromol Chem Macromol Symp 41:55
3. Kausch HH, Heymans N, Plummer CF, Decroly P (2001) Matériaux polymères, propriétés Mécaniques et Physiques. Presses Polytechniques et Universitaires Romandes, Lausanne
4. Michler GH, Balta Calleja FJ (eds) (2005) Mechanical properties of polymer based on nanostructure and morphology, chap. 5.7. Taylor and Francis
5. Khelidj N, Colin X, Audouin L, Verdu J, Monchy-Leroy C, Prunier V (2006) Polym Degrad Stab 91:1593. doi:10.1016/j.polymdegradstab.2005.09.011
6. Richaud E, Farcas F, Bartoloméo P, Fayolle B, Audouin L, Verdu J (2006) Polym Degrad Stab 91:398. doi:10.1016/j.polymdegradstab.2005.04.043
7. Richaud E, Farcas F, Fayolle B, Audouin L, Verdu J (2008) J Appl Polym Sci 110:3313
8. Griffith AA (1920) Philos Trans R Soc Lond A 221:163
9. Celina M, George GA, Lacey DJ, Billingham NC (1995) Polym Degrad Stab 47:311. doi:10.1016/0141-3910(94)00134-T
10. Richters P (1970) Macromolecules 3:262. doi:10.1021/ma60014a027
11. Fayolle B, Audouin L, George GA, Verdu J (2002) Polym Degrad Stab 77:515. doi:10.1016/S0141-3910(02)00110-6
12. Zhang XC, Cameron RE (1999) J Appl Polym Sci 74:2234. doi:10.1002/(SICI)1097-4628(19991128)74:9<2234::AID-APP12>3.0.CO;2-S
13. Brambilla L, Consolati G, Gallo R, Quasso F, Severini F (2003) Polymer 44:1041. doi:10.1016/S0032-3861(02)00904-7
14. Girois S, Audouin L, Verdu J, Delprat P, Marot G (1996) Polym Degrad Stab 51:125. doi:10.1016/0141-3910(95)00166-2
15. Severini F, Gallo R, Ipsale S (1988) Polym Degrad Stab 22:53. doi:10.1016/0141-3910(88)90056-0
16. Fayolle B, Audouin L, Verdu J (2002) Polym Degrad Stab 75:123. doi:10.1016/S0141-3910(01)00211-7
17. Rapoport NYa, Shibriaeva LC, Zaikov VE, Iring M, Fodor ZS, Tüdós F (1985) Polym Degrad Stab 12:191. doi:10.1016/0141-3910(85)90088-6
18. Yakimets-Pilot I (2004) PhD thesis, UTC, Compiegne, France, p 121
19. Gensler R (1998) PhD thesis, EPFL, Lausanne, Switzerland, Nr 1863
20. Kagiya T, Nishimoto S, Watanabe Y, Kato M (1985) Polym Degrad Stab 12:261. doi:10.1016/0141-3910(85)90094-1
21. Viebke J, Elble E, Gedde UW (1994) Polym Eng Sci 36:458
22. Horgh PL, Klemchuck PP (1984) Polym Degrad Stab 8:235
23. Iring M, Tüdós F, Fodor ZS, Kelen T (1980) Polym Degrad Stab 2:143. doi:10.1016/0141-3910(80)90036-1
24. Mendes LC, Rufino ES, de Paula FOC, Torres AC Jr (2003) Polym Degrad Stab 79:371. doi:10.1016/S0141-3910(02)00337-3
25. Suarez JCM, Mano EB, Pereira RA (2000) Polym Degrad Stab 69:217. doi:10.1016/S0141-3910(00)00065-3
26. Fayolle B, Colin X, Audouin L, Verdu J (2007) Polym Degrad Stab 92:231. doi:10.1016/j.polymdegradstab.2006.11.012
27. Fayolle B, Verdu J, Bastard M, Piccoz D (2008) J Appl Polym Sci 107:1783. doi:10.1002/app.26648
28. Sugimoto M, Ishikawa M, Hatada K (1995) Polymer 36:3675. doi:10.1016/0032-3861(95)93769-I
29. Zweifel H (2001) In: Zweifel H (ed) Plastic additives hanbook, 5th edn. Hanser, p 22
30. Fayolle B, Tcharkhtchi A, Verdu J (2004) Polym Test 23:939. doi:10.1016/j.polymertesting.2004.04.013
31. Severini F, Gallo R, Ipsale S (1988) Polym Degrad Stab 22:185. doi:10.1016/0141-3910(88)90041-9
32. Gardner RJ, Martin JB (1977) SPE ANTEC Techn Papers 24:328
33. Greco R, Ragosta G (1987) Plastics Rubber Process Appl 7:163
34. Wu S (1989) J Polym Sci B Polym Phys 27:723. doi:10.1002/polb.1989.090270401
35. Van Krevelen DW (1990) Properties of polymers, 3rd edn. Elsevier, Amsterdam, p 465
36. Plummer CJG (2005) In: Michler GH, Balta-Calleja FJ (eds) Mechanical properties of polymers based on nanostructure and morphology, chap. 6. Taylor and Francis, pp 215–244
37. Tervoort TA, Visjager J, Smith P (2005) Macromolecules 35:8467. doi:10.1021/ma020579g
38. Benkoski JJ, Flores P, Kramer EJ (2003) Macromolecules 36:3289. doi:10.1021/ma034013j
39. Oswald HJ, Turi A (1965) Polym Eng Sci 5:152
40. DiMarzio A, Guttman CM (1980) Polymer 21:733. doi:10.1016/0032-3861(80)90288-8
41. Saito O (1968) J Phys Soc Jpn 13:1451. doi:10.1143/JPSJ.13.1451
42. Kennedy MA, Peacock AJ, Mandelkern L (1994) Macromolecules 27:5297. doi:10.1021/ma00097a009
43. Andrews JM, Ward IM (1970) J Mater Sci 5:411. doi:10.1007/BF00550003
44. Williamson GR, Wright B, Haward RW (1964) J Appl Chem 14:131
45. Popli R, Mandelkern L (1987) J Polym Sci B Polym Phys 25:441. doi:10.1002/polb.1987.090250301
46. Warner SB (1978) J Polym Sci B Polym Phys 16:2139
47. Robelin-Souffache E, Rault J (1989) Macromolecules 22:3581. doi:10.1021/ma00199a015

48. MacMahon W, Birdsall HA, Johnson GR, Camilli CT (1959) J Chem Eng Data 4:57. doi:10.1021/je60001a009
49. Winslow FH, Aloisio CJ, Hawkins WL, Matreyek W, Matsuoka S (1963) Chem Ind Lond 533:1465
50. Winslow FH, Hellman MY, Matreyek W, Skills SM (1966) Polym Eng Sci 6:273
51. Luongo JP (1963) J Polym Sci B Polym Phys 1:141
52. Miyagi A, Wunderlich B (1972) J Polym Sci B Polym Phys 10:2073
53. Ellison S, Fisher LD, Alger KW, Zeronian SH (1982) J Appl Polym Sci 27:247. doi:10.1002/app.1982.070270126
54. Ballara A, Verdu J (1989) Polym Degrad Stab 26:361. doi:10.1016/0141-3910(89)90114-6
55. Wyzgoski MG (1981) J Appl Polym Sci 26:1689. doi:10.1002/app.1981.070260524
56. Mucha M, Kryszewski M (1980) Colloid Polym Sci 258:743
57. Mathur AB, Mathur GN (1982) Polymer (Guildf) 23:54. doi:10.1016/0032-3861(82)90014-3
58. Gensler R, Plummer CJG, Kausch H-H, Kramer E, Pauquet J-R, Zweifel H (2000) Polym Degrad Stab 67:195. doi:10.1016/S0141-3910(99)00113-5
59. Karlsson K, Smith GB, Gedde UW (1992) Polym Eng Sci 32:699
60. Fayolle B, Verdu J, Piccoz D, Dahoun A, Hiver JM, G'sell C, J Appl Polym Sci (in press)
61. Blais P, Carlsson DJ, Wiles DM (1972) J Polym Sci A-1 Polym Chem 10:1077. doi:10.1002/pol.1972.150100412
62. Rabello MS, White JR (1997) Polym Degrad Stab 56:55. doi:10.1016/S0141-3910(96)00202-9
63. Kostoski D, Stojanović Z (1995) Polym Degrad Stab 47:353. doi:10.1016/0141-3910(94)00126-X
64. Sen K, Kumar P (1995) J Appl Polym Sci 55:857. doi:10.1002/app.1995.070550603
65. Zhang RC, Cameron RE (1994) J Appl Polym Sci 74:2234. doi:10.1002/(SICI)1097-4628(19991128)74:9<2234::AID-APP12>3.0.CO;2-S
66. Lassiaz M, Pouyet J, Verdu J (1994) J Mater Sci 29:2177. doi:10.1007/BF01154697
67. Erlandsson B, Karlsson S, Albertsson AC (1997) Polym Degrad Stab 55:237. doi:10.1016/S0141-3910(96)00139-5
68. Liu M, Horrocks AR, Hall ME (1995) Polym Degrad Stab 49:151. doi:10.1016/0141-3910(95)00036-L
69. Quereshi FS, Amin MB, Maadhah AG, Hamid SH (1989) Polym Plast Techn Eng 28:649. doi:10.1080/03602558908049820
70. Papet G, Jirackova-Audouin L, Verdu J (1987) Int J Radiat Appl Instr C Radiat Phys Chem 29:65. doi:10.1016/1359-0197(87)90063-4
71. Langlois V, Meyer M, Audouin L, Verdu J (1992) Polym Degrad Stab 36:207. doi:10.1016/0141-3910(92)90057-C
72. Nitta KH, Tanaka A (2001) Polymer 42:1219. doi:10.1016/S0032-3861(00)00418-3
73. Voigt-Martin IG, Mandelkern L (1984) J Polym Sci B Polym Phys 22:1901
74. Jordens K, Wilkes GL, Janzen J, Rohlfing DC, Welch MB (2000) Polymer 41:7175. doi:10.1016/S0032-3861(00)00073-2
75. Galeski A (2005) In: Michler GH, Balta-Calleja FJ (eds) Mechanical properties of polymers based on nanostructure and morphology, chap. 5. Taylor & Francis, Boca Raton, FL, pp 159–211
76. Henning S, Michler GH (2005) In: Michler GH, Balta-Calleja FJ (eds) Mechanical properties of polymers based on nanostructure and morphology, chap. 7. Taylor & Francis, Boca Raton, FL, pp 245–278
77. Trankner T, Hedenquist M, Gedde UW (1994) Polym Eng Sci 34:1581
78. Bedoui F, Diani J, Régnier G (2004) Polymer (Guildf) 45:2433. doi:10.1016/j.polymer.2004.01.028
79. Capaccio C, Ward IM, Wilding MA, Longman GWJ (1978) J Macromol Sci Phys B25:381
80. Gedde UW, Ifwarson M (1990) Polym Eng Sci 30:202. doi:10.1002/pen.760300403
81. Chaupart N (1995) PhD thesis, Université Pierre et marie Curie, Paris, pp 131–134
82. Men YF, Rieger J, Enderle H-F, Lilge D (2004) Eur Phys J 15:421
83. Peterlin A (1965) J Polym Sci C9:61
84. Seguela R (2005) J Polym Sci B Polym Phys 43:1729. doi:10.1002/polb.20414
85. Krigbaum WR, Roe R-J, Smith KJ (1964) Polymer (Guildf) 5:533. doi:10.1016/0032-3861(64)90202-2
86. Huang Y-L, Brown N (1991) J Polym Sci B Polym Phys 29:129. doi:10.1002/polb.1991.090290116